

Assembly of dysprosium(III) cubanes in metal–organic framework with ecu topology and single-molecule magnetism

Dong Shao, ^{*a} Yi Wan, ^a Jiong Yang, ^c Zhijun Ruan, ^a Junlun Zhu ^a and Le Shi ^{*b}

^a Hubei Key Laboratory of Processing and Application of Catalytic Materials, College of Chemistry and Chemical Engineering, Huanggang Normal University, Huanggang 438000, P. R. China

^b Stoddart Institute of Molecular Science, Department of Chemistry, Zhejiang University, Hangzhou 310027, PR China

^c Department of Chemistry, Southern University of Science and Technology (SUSTech), Shenzhen 518055, China

Correspondence and requests for materials should be addressed to

Email: shaodong@nju.edu.cn

Table of Contents

EXPERIMENTAL SECTION	3
Table S1. Crystallographic data and structure refinement parameters for Dy ₄ -MOF at different measured temperature.....	6
Figure S1. The photograph of a single crystal of Dy₄-MOF	7
Figure S2. The TGA curve of Dy₄-MOF	8
Figure S3. The IR spectra of Dy₄-MOF	9
Figure S4. The asymmetric units of Dy₄-MOF and its model showing atomic displacement parameters (ADPs) without the disorder solvents.	10
Table S2. Continuous Shape Measure (CSM) analysis for eight-coordinated Dy(III) in Dy ₄ -MOF.....	11
Table S3. Selected bond lengths (Å) in Dy ₄ -MOF.	12
Table S4. Selected bond angles (Å) in Dy ₄ -MOF.	13
Figure S5. Portion of the 3D framework structure of Dy₄-MOF along the crystallographically <i>a</i> direction.....	14
Topology analysis of Dy ₄ -MOF	15
Figure S6. Curie-Weiss fit for Dy₄-MOF	16
Figure S7. Frequency dependence of ac susceptibility measured under zero dc field for Dy₄-MOF	17
Figure S8. Temperature dependence of the ac magnetic susceptibility measured under zero dc field for Dy₄-MOF	18
Figure S9. τ^{-1} vs. <i>T</i> for Dy₄-MOF fitted by using proposed models.	19
Figure S10. The <i>M</i> vs. <i>H</i> curve measured at 1.8 K for Dy₄-MOF	20
Table S5. Relaxation fitting parameters from the least-square fitting of the Cole-Cole plots of Dy ₄ -MOF under 0 Oe dc field according to the generalized Debye model.	21
Figure S11. Calculated magnetic anisotropy axes of the Dy(III) ions using MAGELLAN software for Dy₄-MOF	22
References	23

EXPERIMENTAL SECTION

Materials and Synthesis. All reagents were purchased from commercially available sources and used without further purification. The ligands H₄dhbdc was directly bought from TCI chemicals.

Synthesis of {[Dy₄(μ₃-OH)₄(H₂dhbdc)₄(H₂O)₄]·(DMF)₃(H₂O)₃]_n (Dy₄-MOF). The hydrothermal method was employed to synthesize the coordination polymer. A mixture of Dy(NO₃)₃·6H₂O (23mg, 0.05 mmol), H₄dhbdc (20 mg, 0.1 mmol), DMF (1 mL), and water (6 mL) was placed in a 15 mL Teflon-coated stainless steel vessel and heated to 100 °C for 3 days. The vessel was then cooled to room temperature at a rate of 10 °C per hour. Yellow single crystals of **Dy₄-MOF** were collected, with a yield of 52% (based on Dy³⁺). Elemental analysis calcd. (%) for C₄₁H₅₅Dy₄O₃₈N₃ (include DMF and H₂O): C, 26.64; H, 3.00; N, 2.27. Found: C, 26.81, H, 2.53; N, 2.21. IR (KBr, cm⁻¹, Figure S3): 3500-3000 (bs), 1656(s), 1544(w), 1445(s), 1113(vs), 783(w) cm⁻¹.

Physical measurements

Infrared spectra (IR) data were measured on KBr pellets using a Nexus 870 FT-IR spectrometer in the range of 4000-400 cm⁻¹. Elemental analyses of C, H, and N were performed at an Elementar Vario MICRO analyzer. Powder X-ray diffraction data (PXRD) were recorded on a Bruker D8 Advance diffractometer with Cu Kα X-ray source (λ = 1.54056 Å) operated at 40 kV and 40 mA. Thermal gravimetric analysis (TGA) was measured in Al₂O₃ crucibles using a PerkinElmer Thermal Analysis in the temperature range of 30-800 °C under an argon atmosphere.

Magnetic measurements

Magnetic measurements from 2 to 300 K with applied direct current (dc) field up to 7 T were performed using a Quantum Design VSM and PPMS magnetometer on the

crushed samples from the single crystals of the compound. Alternative current (ac) magnetic susceptibility data were collected in a zero-dc field or an applied 1000 Oe dc fields in the temperature range of 2-8 K. All magnetic data were corrected for the diamagnetic contributions of the sample holder and of core diamagnetism of the sample using Pascal's constants.

X-ray Crystallography

Single crystal X-ray diffraction data were collected on a Bruker D8 QUEST diffractometer with a PHOTON III area detector (Mo-K α radiation, $\lambda = 0.71073 \text{ \AA}$, Bruker *Ius* 3.0) at 100 K. The APEX III program was used to determine the unit cell parameters and for data collection. The data were integrated and corrected for Lorentz and polarization effects using SAINT.^{S1} Absorption corrections were applied with SADABS.^{S2} The structures were solved by direct methods and refined by full-matrix least-squares method on F^2 using the SHELXTL^{S3} crystallographic software package integrated in Olex 2.^{S4} All the non-hydrogen atoms were refined anisotropically. Hydrogen atoms of the organic ligands were refined as riding on the corresponding non-hydrogen atoms. SADABS-2016/2 (Bruker, 2016/2) was used for multi-scan absorption correction. The minimum of transmission is 0.0199, the maximum of transmission is 0.0453 and the ratio of minimum to maximum transmission is 0.4393, all of them are relatively small values. Notably, there are two H atoms were not added. Additional details of the data collections and structural refinement parameters are provided in Table 1. Selected bond lengths and angles of **Dy₄-MOF** were listed in Table S1 and S2. CCDC 2179379 are the supplementary crystallographic data for this

paper. They can be obtained freely from the Cambridge Crystallographic Data Centre via www.ccdc.cam.ac.uk/data_request/cif.

Table S1. Crystallographic data and structure refinement parameters for **Dy₄-MOF** at different measured temperature.

Complex	Dy₄-MOF
Empirical formula	C ₃₂ H ₂₀ Dy ₄ O ₃₂
Formula weight	1566.48
<i>T</i> / K	281
Crystal system	monoclinic
Space group	<i>P</i> 2 ₁ /m
<i>a</i> /Å	13.442(4)
<i>b</i> /Å	21.256(6)
<i>c</i> /Å	17.195(5)
α /°	90
β /°	108.984
γ /°	90
Volume/Å ³	4646(2)
<i>Z</i>	2
ρ_{calc} g/cm ³	1.564
μ /mm ⁻¹	3.332
F(000)	2144.0
2 Θ range for data collection/°	3.93 to 53.178
Reflections collected	34784
Independent reflections	9459
<i>R</i> _{int} / <i>R</i> _{sigma}	0.0620 / 0.0628
Goodness-of-fit on <i>F</i> ²	0.994
<i>R</i> ₁ ^a / <i>wR</i> ₂ ^b (<i>I</i> > 2 σ (<i>I</i>))	0.0391 / 0.1070
<i>R</i> ₁ / <i>wR</i> ₂ (all data)	0.0508 / 0.1122
Max/min [e Å ⁻³]	1.21/-1.21
^a <i>R</i> ₁ = $\sum F_o - F_c / \sum F_o $ ^b <i>wR</i> ₂ = $\{\sum[w(F_o^2 - F_c^2)^2] / \sum[w(F_o^2)^2]\}^{1/2}$	

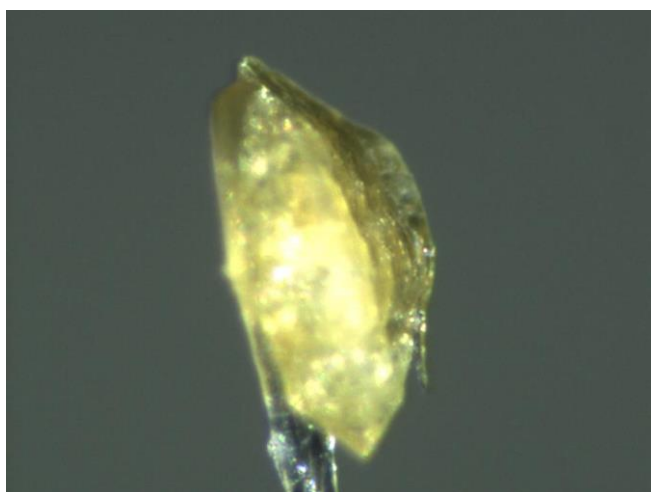


Figure S1. The photograph of a single crystal of **Dy₄-MOF**.

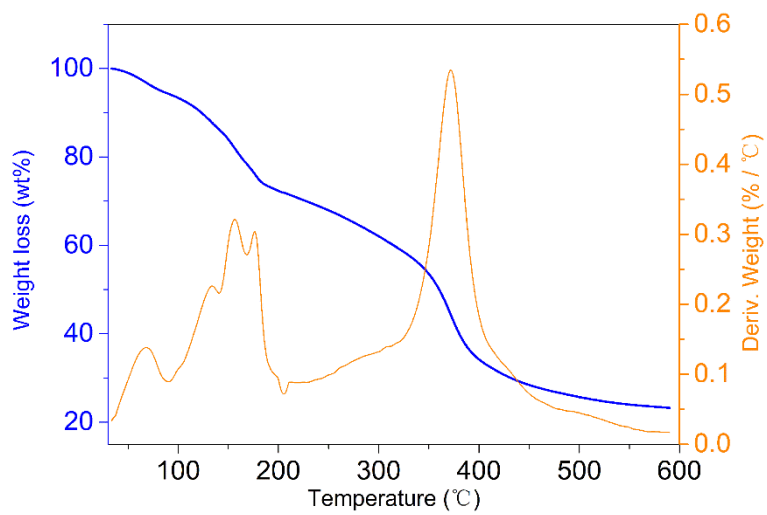


Figure S2. The TGA curve of Dy₄-MOF.

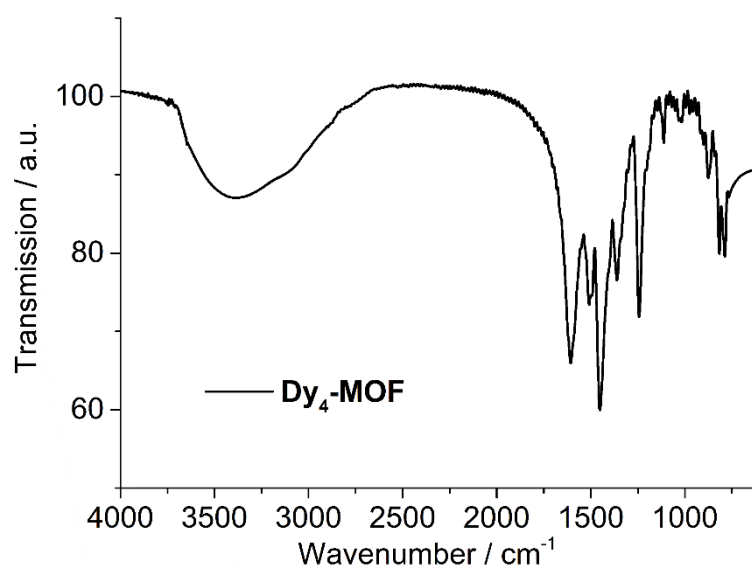


Figure S3. The IR spectra of **Dy₄-MOF**.

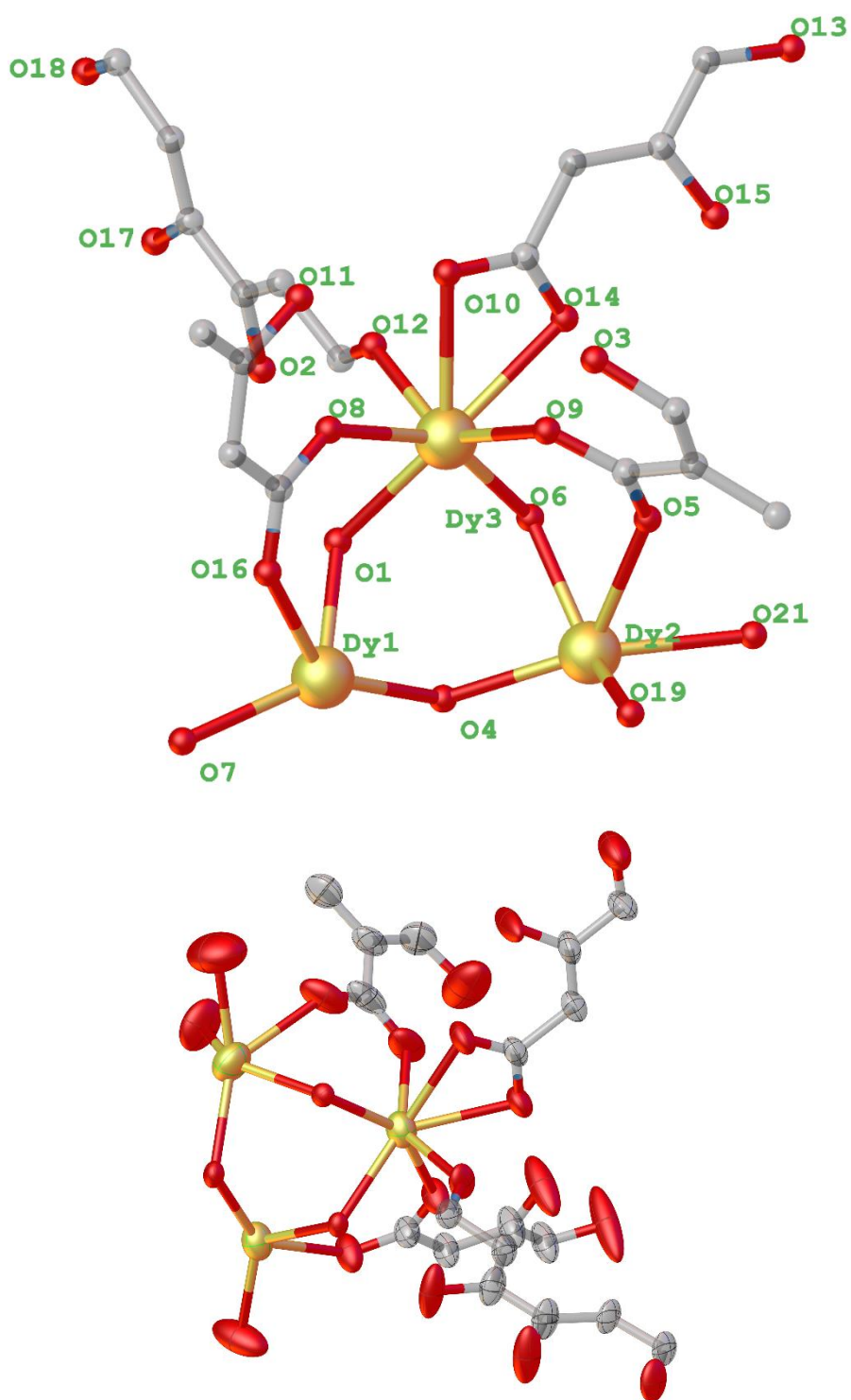


Figure S4. The asymmetric units of **Dy₄-MOF** and its model showing atomic displacement parameters (ADPs) without the disorder solvents.

Table S2. Continuous Shape Measure (CSM) analysis for eight-coordinated Dy(III) in Dy₄-MOF.

Eight-coordinated coordination sphere label	Shape	CSM parameters			Determined coordination geometry
		Dy1	Dy2	Dy3	
OP-8	Octagon	29.947	29.547	28.000	
HPY-8	Heptagonal pyramid	22.216	23.629	21.807	
HBPY-8	Hexagonal bipyramid	17.076	16.501	13.679	
CU-8	Cube	11.315	11.387	11.736	
SAPR-8	Square antiprism	1.221	1.157	2.461	SAPR-8
TDD-8	Triangular dodecahedron	3.676	2.001	1.633	TDD-8
JGBF-8	Johnson - Gyrobifastigium (J26)	16.229	14.124	12.036	
JETBPY-8	Johnson - Elongated triangular bipyramid (J14)	26.963	28.107	27.483	
JBTP-8	Johnson - Biaugmented trigonal prism (J50)	3.547	1.797	2.162	
BTPR-8	Biaugmented trigonal prism	2.386	1.273	1.636	BTPR-8
JSD-8	Snub disphenoid (J84)	6.443	4.223	2.625	
TT-8	Triakis tetrahedron	11.946	12.071	12.523	
ETBPY-8	Elongated trigonal bipyramid (see 8)	22.357	23.544	24.167	

Table S3. Selected bond lengths (Å) in **Dy₄-MOF**.

Bond	Lengths (Å)	Bond	Lengths (Å)	Bond	Lengths (Å)
Dy1-O1	2.328(4)	Dy2-O4	2.359(3)	Dy3-O1	2.387(3)
Dy1-O4	2.359(3)	Dy2-O4 ¹	2.359(3)	Dy3-O4 ¹	2.402(3)
Dy1-O4 ¹	2.359(3)	Dy2-O5 ¹	2.412(5)	Dy3-O6	2.336(3)
Dy1-O16 ¹	2.350(4)	Dy2-O5	2.412(5)	Dy3-O8	2.276(3)
Dy1-O16	2.350(4)	Dy2-O6	2.388(4)	Dy3-O9	2.377(4)
Dy1-O18 ²	2.454(4)	Dy2-O19 ¹	2.387(5)	Dy3-O10	2.472(3)
Dy1-O18 ³	2.454(4)	Dy2-O19	2.387(5)	Dy3-O12	2.344(3)
Dy1-O7	2.349(7)	Dy2-O21	2.365(8)	Dy3-O14	2.446(4)
Dy1/O _{average}	2.375	Dy2/O _{average}	2.384	Dy3/O _{average}	2.380
Dy1-Dy2	3.8673(9)	Dy1-Dy3	3.8199(6)	Dy1-Dy3 ¹	3.8200(6)
Dy2-Dy3	3.6980(5)	Dy2-Dy3 ¹	3.6980(5)	Dy3-Dy3 ¹	3.7382(8)
¹ +X,1/2-Y,+Z; ² 1+X,+Y,+Z; ³ 1+X,1/2-Y,+Z					

Table S4. Selected bond angles (Å) in **Dy₄-MOF**.

Parameter	bond angles (Å)
Dy3 ¹ -Dy1-Dy2	57.504(10)
Dy3-Dy1-Dy3 ¹	58.589(14)
Dy1-O1-Dy3	108.24(12)
Dy3-O1-Dy3 ¹	103.10(16)
Dy1-O4-Dy3 ¹	106.71(12)
Dy2-O4-Dy1	110.08(13)
Dy2-O4-Dy3 ¹	101.92(12)
Dy3-O6-Dy2	103.02(13)
Dy3-O6-Dy3 ¹	106.28(17)
O1-Dy1-O4	70.39(11)
O1-Dy1-O16	83.91(11)
O1-Dy1-O7	126.7(3)
O4-Dy1-O4 ¹	68.07(15)
O16 ¹ -Dy1-O4	78.47(13)
O16-Dy1-O4 ¹	78.47(13)
O7-Dy1-O4 ¹	143.90(12)
O7-Dy1-O16	73.13(14)
O19-Dy1-O19 ¹	70.2(3)
O21-Dy2-O5	71.64(19)
O21-Dy2-O6	99.5(4)
O1-Dy3-O10	137.15(13)
O1-Dy3-O14	140.93(13)
O9-Dy3-O1	141.14(15)
O9-Dy3-O10	72.48(15)
O12-Dy3-O9	143.16(14)
¹ 1-X,1-Y,-Z; ² 1-X,1-Y,1-Z	

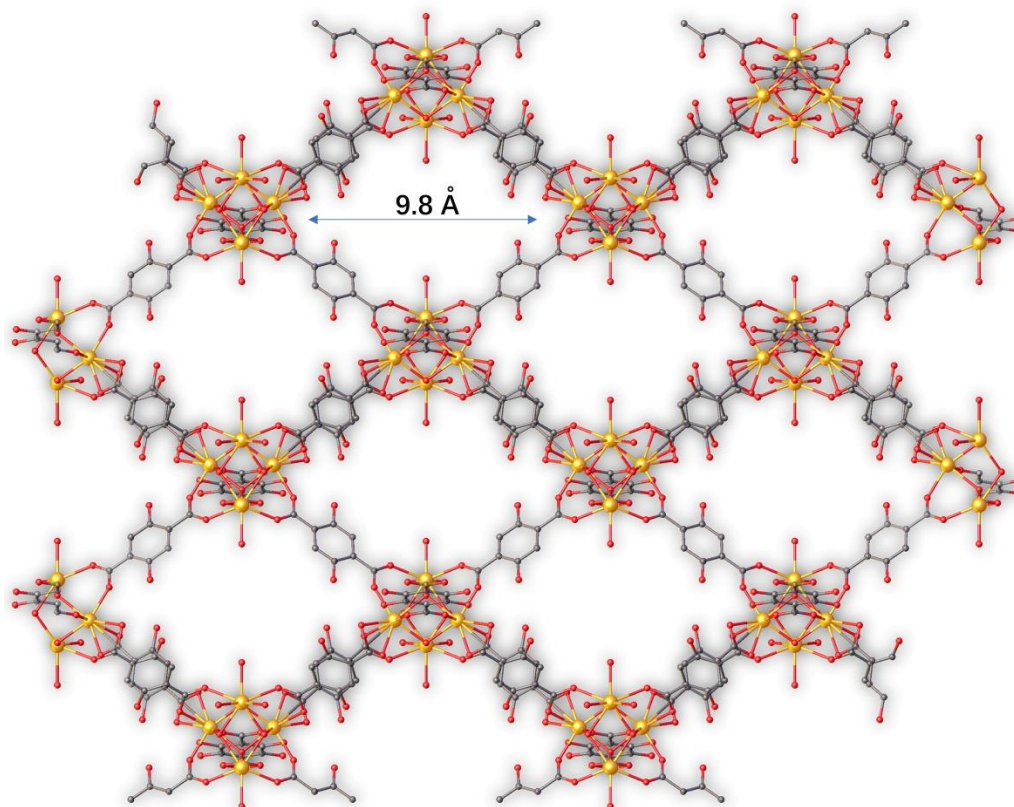
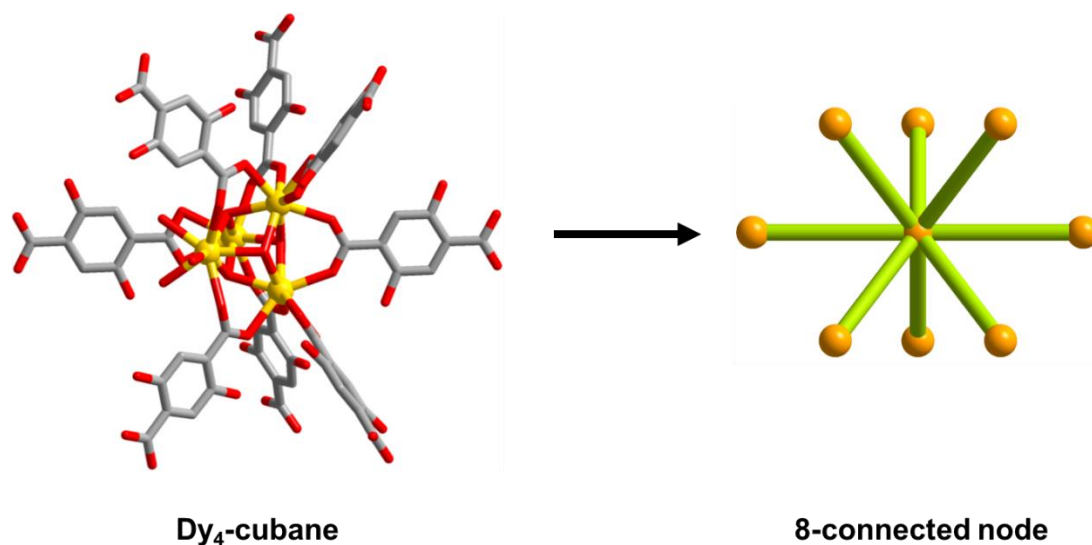


Figure S5. Portion of the 3D framework structure of **Dy₄-MOF** along the crystallographically *a* direction.

Topology analysis of Dy₄-MOF



Prior to topological analysis, the structure has been simplified to its points of extension.

The cubane cluster is then reduced to an 8-connected node (α)

The Dy₄-MOF exhibits an 8-connected **ecu** topology.

Point symbol for net: $3^6.4^{15}.5^7$; 8-c uninodal net

Topological terms for each node:

(α) Point symbol: $3^6.4^{15}.5^7$.

Extended point symbol:

3.3.3.3.3.3.4.4.4.4.4.4.4.4(2).4(2).4(2).5(5).5(5).4.4.4.4.5.5.5.5(2)

Coordination sequences: 8 28 60 106 164 236 320 418 528 652

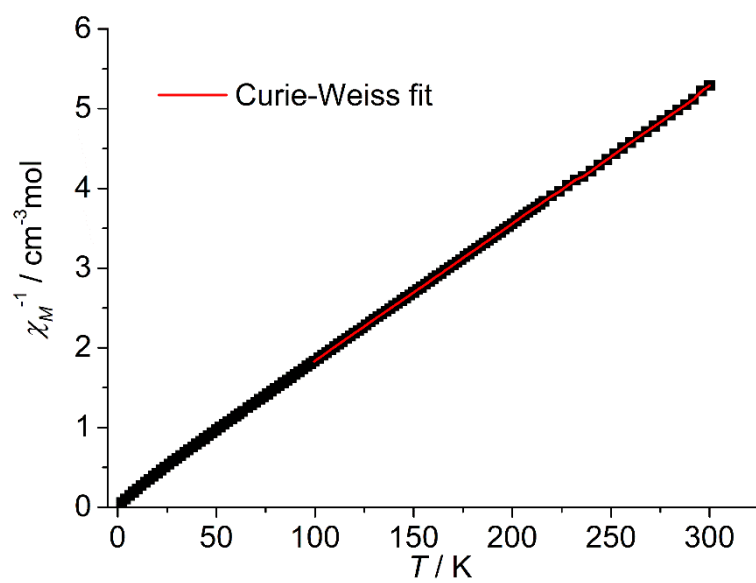


Figure S6. Curie-Weiss fit for **Dy₄-MOF**.

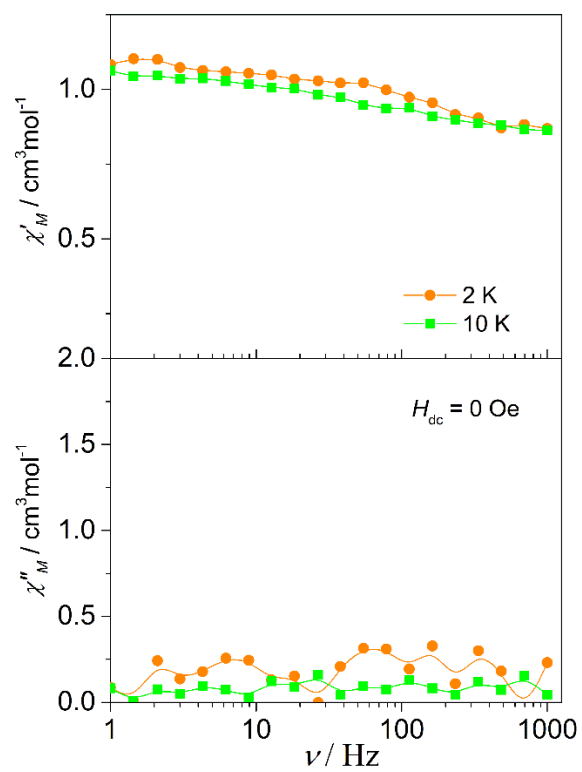


Figure S7. Frequency dependence of ac susceptibility measured under zero dc field for Dy₄-MOF.

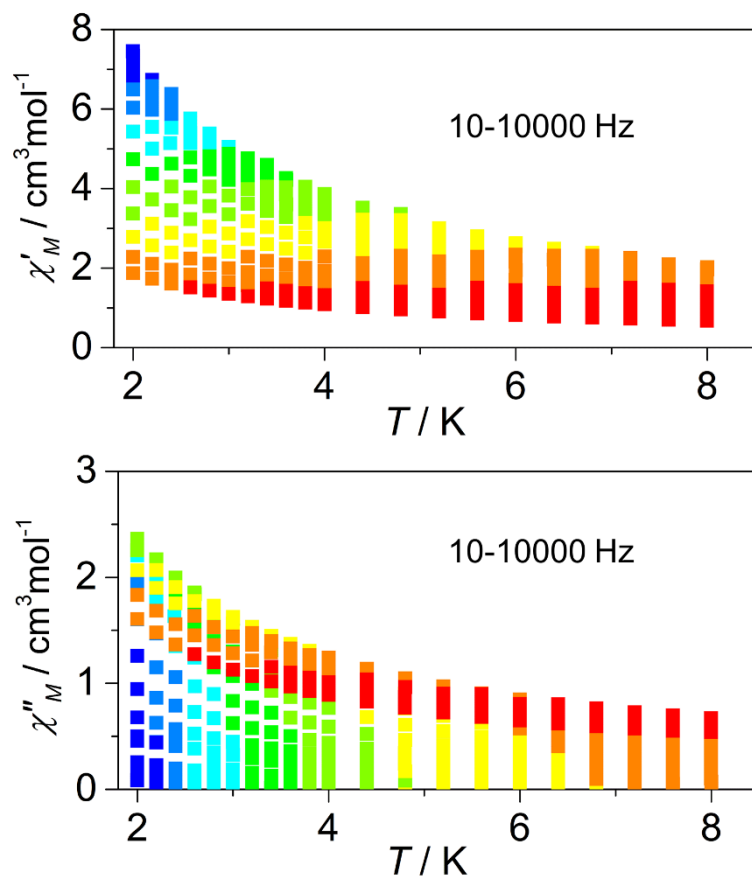


Figure S8. Temperature dependence of the ac magnetic susceptibility measured under zero dc field for $\text{Dy}_4\text{-MOF}$.

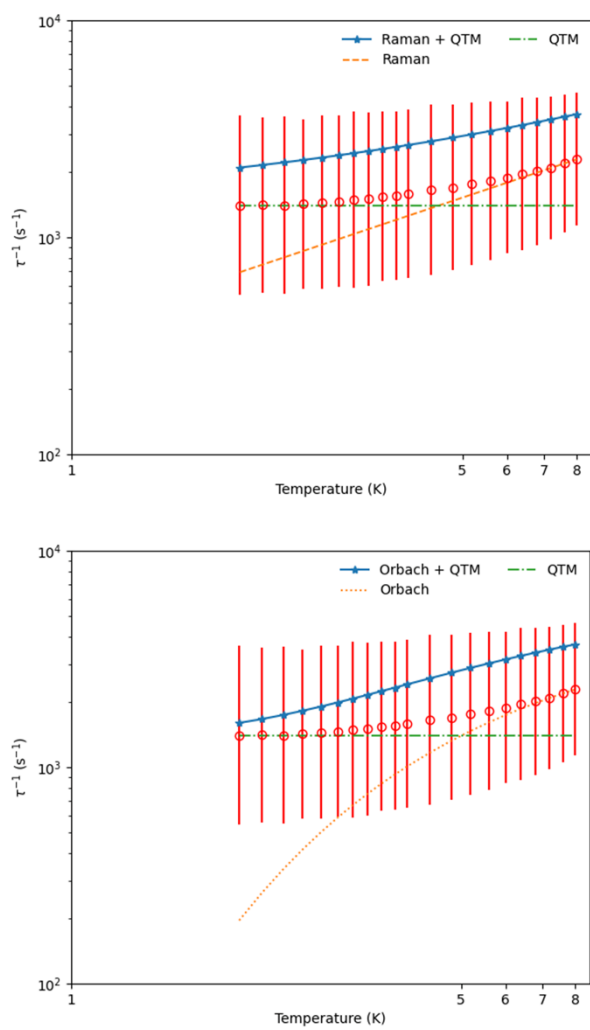


Figure S9. τ^{-1} vs. T for $\text{Dy}_4\text{-MOF}$ fitted by using proposed models.

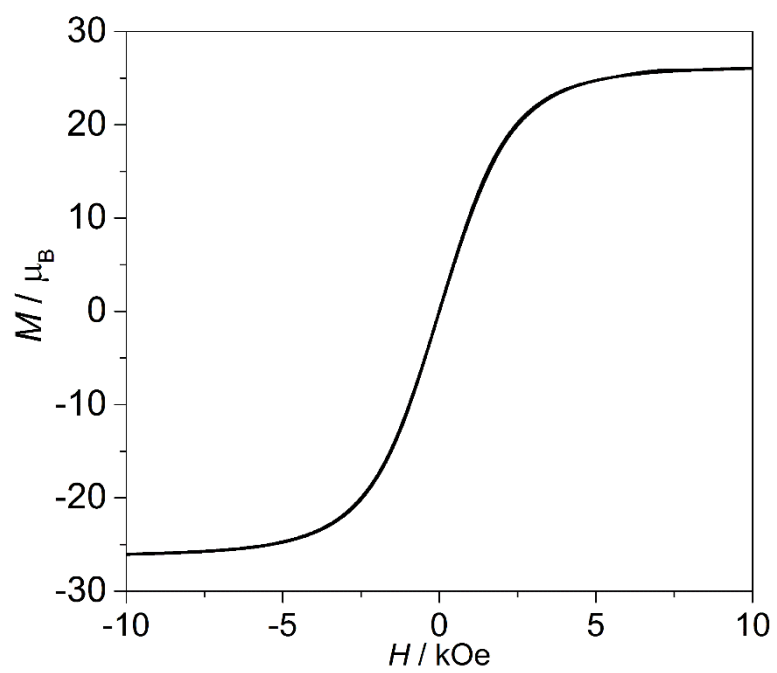


Figure S10. The M vs. H curve measured at 1.8 K for **Dy₄-MOF**.

Table S5. Relaxation fitting parameters from the least-square fitting of the Cole-Cole plots of **Dy₄-MOF** under 0 Oe dc filed according to the generalized Debye model.

T / K	τ / s	χ_S / cm ³ mol ⁻¹ K	χ_T / cm ³ mol ⁻¹ K	α
2.00005	7.11676E-4	0.92688	7.16538	0.18288
2.20009	7.09302E-4	0.884	6.57072	0.17765
2.39948	7.1265E-4	0.83033	6.09784	0.17968
2.60018	7.031E-4	0.80983	5.63089	0.16934
2.80014	6.89681E-4	0.7414	5.25428	0.17355
3.00009	6.82004E-4	0.70684	4.93102	0.17211
3.20019	6.70074E-4	0.64907	4.6546	0.17868
3.40022	6.64366E-4	0.63505	4.40419	0.17434
3.60003	6.483E-4	0.61441	4.14927	0.16803
3.8002	6.40623E-4	0.59404	3.95049	0.1669
4.00006	6.2949E-4	0.56474	3.76895	0.16853
4.40003	6.03705E-4	0.51251	3.43961	0.16996
4.79999	5.90096E-4	0.49717	3.17428	0.16266
5.19997	5.66238E-4	0.4654	2.93007	0.15859
5.59995	5.48872E-4	0.44495	2.7283	0.15346
5.99991	5.29865E-4	0.42972	2.54456	0.14416
6.39987	5.11739E-4	0.40213	2.39805	0.14457
6.79984	4.96419E-4	0.38815	2.26622	0.13862
7.19984	4.78924E-4	0.37669	2.14124	0.12965
7.59978	4.56558E-4	0.35682	2.02827	0.1242
7.99982	4.37253E-4	0.34405	1.93018	0.11681

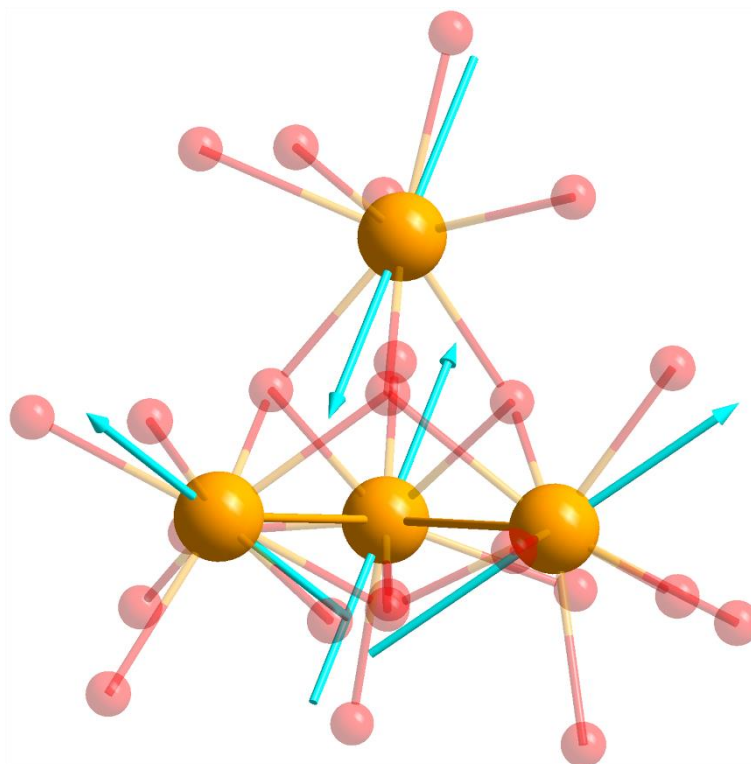


Figure S11. Calculated magnetic anisotropy axes of the Dy(III) ions using MAGELLAN software for **Dy₄-MOF**.

References

- 1) SAINT Software Users Guide, version 7.0; Bruker Analytical X-Ray Systems: Madison, WI, 1999.
- 2) G. M. Sheldrick, SADABS, version 2.03; Bruker Analytical X-Ray Systems, Madison, WI, 2000.
- 3) G. M. Sheldrick, SHELXTL, Version 6.14, Bruker AXS, Inc.; Madison, WI 2000-2003.
- 4) Dolomanov, O. V.; Bourhis, L. J.; Gildea, R. J.; Howard, J. A. K.; Puschmann, H. OLEX2: A Complete Structure Solution, Refinement and Analysis Program. *J. Appl. Crystallogr.*, 2009, 42, 339–341.